Proceedings of the Sixth International Conference on
Railway Technology: Research, Development and Maintenance
Edited by: J. Pombo
Civil-Comp Conferences, Volume 7, Paper 2.5
Civil-Comp Press, Edinburgh, United Kingdom, 2024
ISSN: 2753-3239, doi: 10.4203/ccc.7.2.5

Wheel/Rail Adhesion and Coefficient of Friction Measurement using Downscaled Test Rig

G. Jayasree Krishnan, Z. Yang and Z. Li

Department of Engineering Structures, Faculty of CEG, Delft University of Technology
the Netherlands

Abstract

Creep curves characterise the behaviour of frictional forces at the wheel-rail interface. This study used the V-Track test rig to measure lateral and longitudinal creep curves under clean and dry contact conditions with practical wheel-rail contact pressures. The measured lateral and longitudinal creep curves were cross-compared to estimate the coefficient of friction of the V-Track. The measurement results and findings demonstrate the reliability of using the V-Track test rig to study the wheel-rail frictional rolling contact and to accurately measure the coefficient of friction at the wheel-rail interface, highlighting its significance in railway engineering and operational safety studies.

Keywords: coefficient of friction, creep curve, V-Track test rig, comparison, torque, angle of attack.

1 Introduction

Wheel-rail friction (and adhesion) influences all aspects of railway operations as trains rely on the friction between the wheel and rail for guidance, stability, traction and braking. Safety consequences such as Signals Passed at Danger (SPADs) [1], and wheel slips may result from insufficient friction. Frictional forces (or creep forces) acting in the rolling contact wheel-rail interface originate from relative velocities and deformations of contacting points on the wheel and rail (termed creepage) and can be influenced by a variety of factors such as the surface roughness, normal load, presence of a third-body layer, etc [2, 3, 4]. The relationship between the creep forces and

creepage is characterised by the creep curve. Thus, the measurement of creep curves under different contact conditions is vital for the characterisation of wheel-rail friction behaviour.

Creep curves measured using real trains on service tracks give the most accurate reflection of wheel-rail friction behaviour. However, field creep curve measurements are often prohibitively expensive and can cause additional damage to tracks. Due to these reasons, creep curve measurements are often conducted in the laboratory under controlled conditions using either full-scale or reduced-scale test rigs. Among the latter, the twin-disc setup is the most common [1, 5, 6], where the wheel and rail are represented by two cylindrical discs pressed together. These are cheaper and easier to operate in contrast to the full-scale roller rigs [3, 7, 8], which consists of a real-life wheel or wheelset pressed onto discs that have the same profile as the rail. However, in both these setups, pure lateral creep curve measurements can be challenging, as reflected in the very low number of publications concerning lateral creep curve measurements [9, 10]. Further, there has been no study, to the authors' knowledge, which validates the measured coefficient of friction by a cross-comparison of both the longitudinal and lateral creep curves measured from the same test rig.

This study uses the V-Track test rig to measure both the lateral and longitudinal creep curves under clean and dry contact conditions. The V-Track test rig is able to accurately and independently control the angle of attack (AoA) and torque on the wheels. This enables both pure lateral creepage and pure longitudinal creepage conditions to be reproduced. Additionally, V-Track is capable of maintaining similar dynamic characteristics and levels of normal contact pressure to the real-life wheel-rail contact. The measured lateral and longitudinal creep curves were then cross-compared with each other to assess the reliability of measuring the coefficient of friction using V-Track.

2 Test Procedure

The V-Track test rig consists of a ring track on which a maximum of four wheel assemblies can run, as shown in Figure 1. The ring track was made using four pieces of rails with a custom rail profile derived from 1:5 scaled 54E1 rail profile [11]. These were each bent into an arc covering 90 degrees and then connected by joints. The rails were fixed onto 100 equally spaced sleepers with rail pads mounted in between throughout the circumference of the ring track. Rubber pads were laid underneath the sleepers to simulate the stiffness and damping of a ballast layer. In the configuration used for the present work, only two wheel assemblies were present. Each wheel assembly (also shown in Figure 1) was mounted to a rigid steel frame, that extends to the centre of the ring track, and forms a platform that can be rotated by a motor and pull the wheels along the ring track. Additionally, the wheels were also connected to a second motor which can apply braking or traction torques to the wheels. Two vertical springs within the wheel assembly enable the normal load to be set at the desired value. The wheels were connected to the vertical springs through axle boxes and guiding blocks. The guiding blocks enable the wheels to move vertically, thus maintaining continuous contact with the ring track. The AoA can be adjusted by

pivoting the wheel and axle box with respect to the guiding block within the wheel assembly. This was measured using a dial gauge, which measures the distance rotated by a steel beam attached to the axle box pivot. The steel beam has a length of 68.45 mm, which translates to a rotation angle of 0.08° for every 1mm of dial gauge reading. A four-sensor piezoelectric dynamometer system was placed in between the wheel assembly and the steel frame, which measures the wheel-rail contact forces in three directions. The translational velocity of the wheel was controlled to a constant value by setting the rotational velocity of the platform. The rotational velocity of the wheel was measured by an encoder placed in line with the constant velocity shaft. A more detailed description of the design, contact force, and AoA measurement capabilities of the V-Track test rig can be found in [12], [13] and [9] respectively. For the present study, the nominal normal load for the two wheels was set at 2700 N, which would give a maximum wheel-rail contact pressure of 1.2 GPa. This is representative of the contact pressure between the wheel tread and rail head for passenger trains in the Netherlands. AoA and traction/braking torque were only applied to one wheel (W1) to obtain the best control. The other wheel (W3) is allowed to roll freely, to provide a balance of the normal loads on the test rig. The translational velocity of the wheel was set at 4 km/h.

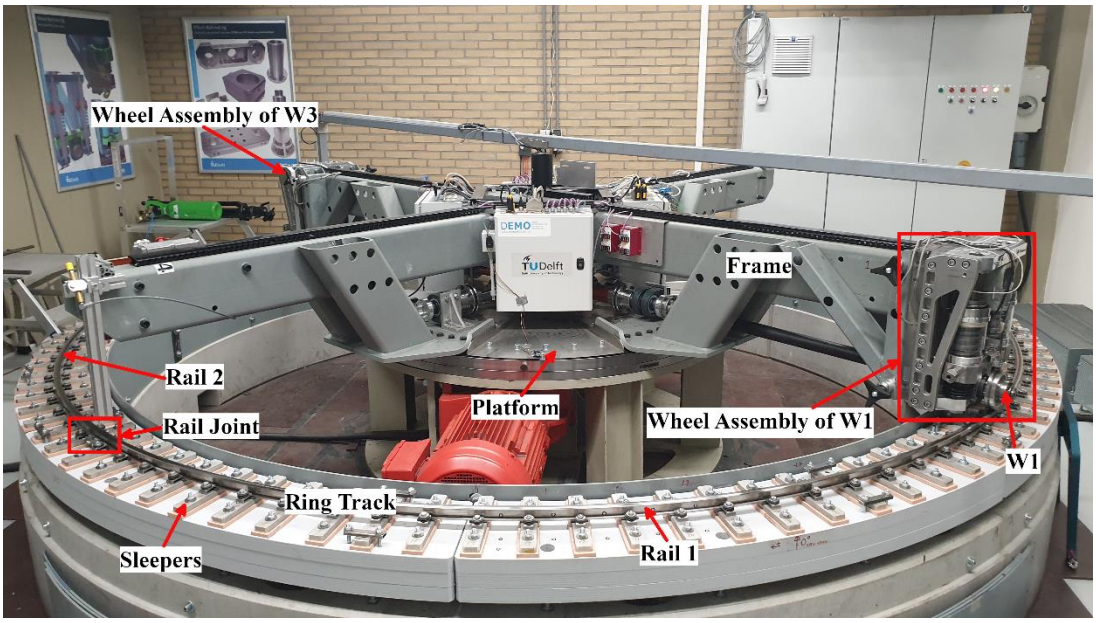

Figure 1: An overview of the V-Track test rig.

For the lateral creep curve test, the AoA of the wheel was increased from 0° to 0.32° in steps of 0.08°. The increment was reduced to 0.04° afterwards to capture more data points in the non-linear part of the creep curve before saturation. For each angle step, the wheel-rail contact forces were recorded for at least 3 cycles. In each cycle, the torque applied to W1 was carefully controlled to provide nominally zero longitudinal wheel-rail contact force, such that pure lateral creepage contact conditions could be maintained along the ring track. The AoA was increased until the friction saturation was observed, indicated by the recorded lateral force remaining approximately constant for further increase in AoA. For each AoA increment, the

coefficient of adhesion (CoA), i.e., the ratio between the friction force and normal load, was calculated from Equation (1):

$$CoA = \frac{\sqrt{F_x^{\,2} + F_y^{\,2}}}{F_z} \tag{1}$$

where F_x, F_y and F_z represent the mean values of the measured longitudinal, lateral and vertical forces respectively. The saturation value of the CoA was taken as the approximate coefficient of friction (CoF) of the V-Track. The rails and wheels were cleaned with acetone before each AoA increment to maintain clean and dry contact conditions throughout the test. The lateral creepage ξ_y was calculated using Equation (2):

$$\xi_y = \sin(AoA) \tag{2}$$

For the longitudinal creep curve test, the AoA of the wheel was set as close as possible to zero, to produce nominally zero lateral wheel-rail contact force and thus pure longitudinal creepage contact conditions. Based on the approximate value of the CoF measured from the lateral creep curve test, the traction torque that may induce friction saturation was estimated as 69 Nm. The traction torque applied to W1 was then increased gradually from zero to 60 Nm with steps of 20 Nm, and then with steps of 3 Nm till 69 Nm to better capture the non-linear portion of the creep curve. The traction torque was not increased further to prevent the possibility of wheel spin out. For each torque step, the wheel-rail contact forces and the wheel and platform rotational speeds were recorded for at least 3 cycles. After every three torque steps, the rails and wheels were cleaned with acetone to maintain clean and dry contact conditions throughout the test. For each torque step, the CoA for the longitudinal creep curve test was also calculated using Equation (1). The longitudinal creepage ξ_x can be calculated using Equation (3):

$$\xi_x = \frac{\Omega R_p - \omega R_w}{\Omega R_p} \tag{3}$$

where Ω represents the rotational speed of the platform, R_p represents the radius of the platform (which is 2.0 m), ω represents the wheel rotational speed measured when the aforementioned torque values were applied, and R_w represents the radius of the wheel, which is 65 mm. However, the accuracy of the encoder measuring the wheel rotational speed was much higher compared to the accuracy of the encoder measuring the platform rotational speed. Thus, a different approach was used to calculate longitudinal creepage, using Equation (4):

$$\xi_x = \frac{\omega_0 R_w - \omega R_w}{\omega_0 R_w} \tag{4}$$

where ω_0 represents the rotational speed of W1 when the measured longitudinal force is nominally zero, i.e., under a free-rolling condition. In this condition, the longitudinal creepage is nominally zero, which implies that $\Omega R_p = \omega_0 R_w$. Since the platform velocity is kept nominally constant throughout the entire test, $\omega_0 R_w$ can be used in place of ΩR_p.

3 Results and Discussions

The measured lateral creep curve is presented first, followed by the measured longitudinal creep curve. The lateral and longitudinal creep curves are then cross-compared with each other, to validate the reliability of V-Track in measuring the CoF.

3.1 Lateral creep curve

The measured lateral creep curve is shown in Figure 2. For each point in the creep curve, a vertical error bar denotes the variation in CoA measured in the repeated cycles at that creepage point. The vertical error bar length corresponds to 50 times the standard deviation of measured CoA values. Such a high multiple of the standard deviation was used to make the error bars more distinct and visible in the plot. If the length had been chosen as the standard deviation, the error bars would have been imperceptibly small and overlapping. Even at such a high multiple, we can see that the error bars are of short length, denoting excellent repeatability of the CoA measurements in the lateral creep curve test. The shaded region in light red extending above and below the points in the plotted creep curve represents the expanded uncertainty to 95% coverage. As can be seen from Figure 2, the lateral creep curve does not start at zero CoA. That can be due to a small angle of attack that was not able to be measured and not able to be made zero during the adjustment.

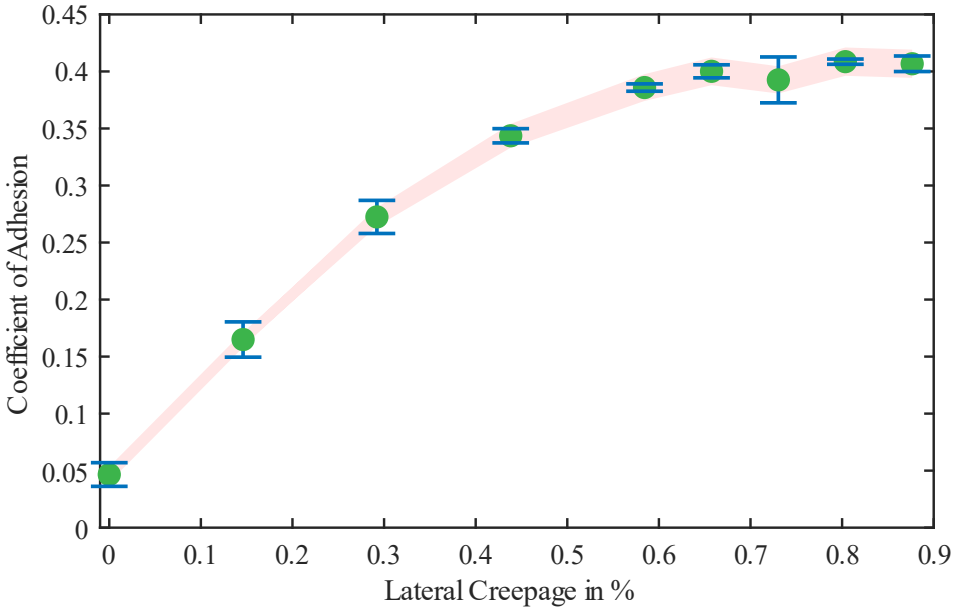

Figure 2: The measured lateral creep curve from V-Track.

3.2 Longitudinal creep curve

The measured longitudinal creep curve is plotted in Figure 3. Here, both the vertical and horizontal error bars are plotted, denoting the variations in the CoA and longitudinal creepage with repeated cycles at each point. The vertical error bar length corresponds to 20 times (to make the bars visible in the plot) of the standard deviation of the measured CoA values, while the horizontal error bar length corresponds to twice the standard deviation of the measured creepage values. The shaded region in light red extending above and below the points in the plotted creep curve represents the expanded uncertainty to 95% coverage. We can see that similar to the lateral creep curve, the vertical error bars are small, representing excellent repeatability of the CoA measurement in the V-Track.

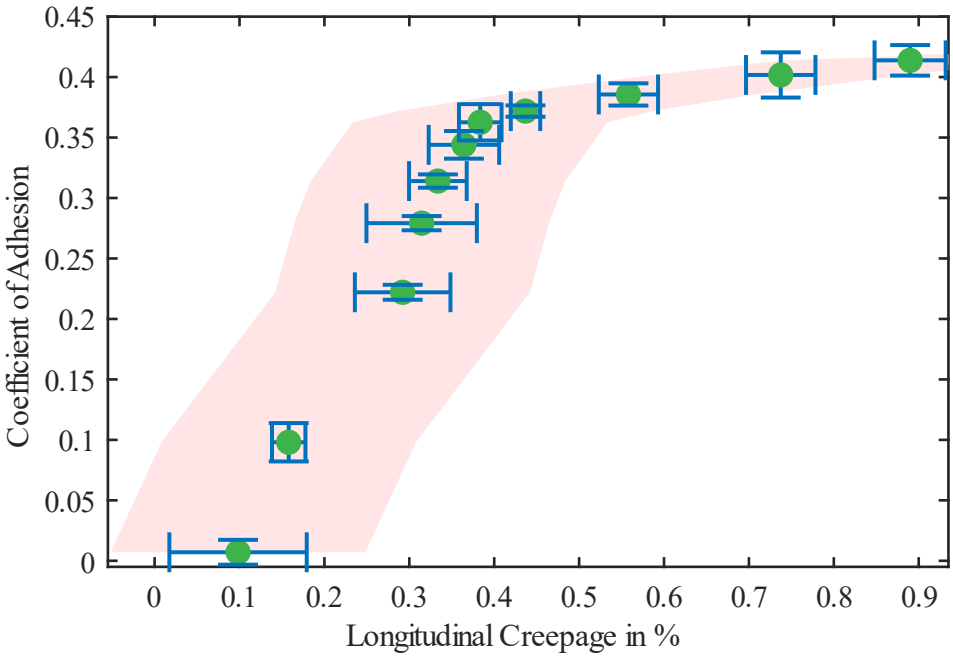

Figure 3: The measured longitudinal creep curve from V-Track.

The difference in the error bar scales and the larger lengths of the horizontal error bars indicate the high variability observed in the measured longitudinal creepage compared to the measured CoA. Another observation is that the longitudinal creep curve does not start at zero creepage. The CoA value is very close to zero, but the initial point is shifted to the right by a significant amount. These observations are due to inaccuracies in the longitudinal creepage measurement at very low creepage values (<0.4%). Accurate measurement of very low values of longitudinal creepage is challenging and relies on the accuracy of the encoder used for wheel rotational speed measurements. The V-Track wheel rotational speed measurement encoder used in this study is insufficiently accurate for this task. Therefore, high variation in the measured longitudinal creepage with repeated cycles is observed, especially in the low creepage range, producing longer horizontal error bars. The measurement inaccuracy is more pronounced when the creepage value is smaller than 0.4%, as indicated by the wider shaded region of uncertainty. It can be seen that, beyond 0.4% creepage, the

uncertainty is reduced considerably, as indicated by a narrower shaded band. Thus, the points after 0.4% creepage can be considered as accurate.

3.3 Cross-comparison of lateral and longitudinal creep curves

In principle, a pure longitudinal creep curve, and a pure lateral creep curve obtained with the same contact geometry, contact body materials and normal load, should saturate at the same CoF value. Thus, by a cross-comparison of the measured lateral and longitudinal creep curves, we can assess the reliability and accuracy of V-Track for CoF measurement. Figure 4 compares the lateral and longitudinal creep curves measured from V-Track. The uncertainty ranges of the curves have been omitted to increase the legibility. The CoFs obtained from the lateral and longitudinal creep curves are 0.4067 and 0.4138, respectively. Thus, a very good agreement is observed with a percentage difference of only 1.7%. These results indicate that the V-Track test rig can reliably measure the CoF from both longitudinal and lateral creep curve tests.

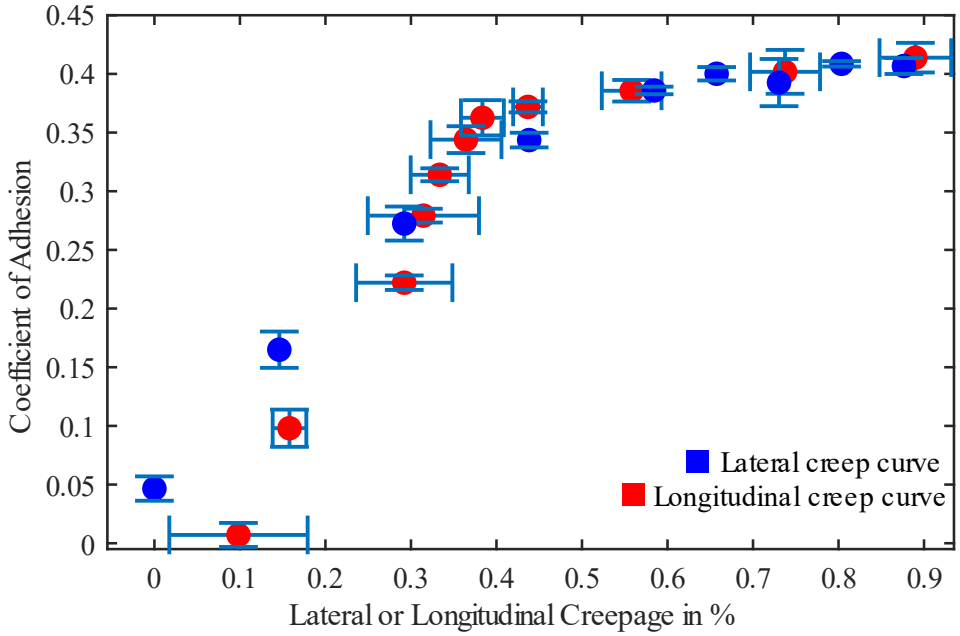

Figure 4: A cross-comparison of the measured lateral and longitudinal creep curves.

4 Conclusions

The V-Track test rig was used in this study to obtain the lateral and longitudinal creep curves under clean and dry contact conditions. Pure lateral creepage and longitudinal creepage conditions were produced by careful control of the longitudinal and lateral contact forces. Friction saturation was induced in the lateral and longitudinal creep curve tests by increasing the AoA, and the applied traction torque, respectively. The capability of the V-Track test setup in measuring the CoF at the wheel-rail interface was assessed by a cross-comparison of the measured lateral and longitudinal creep curves. The CoF of V-Track under clean and dry conditions was measured to be about 0.41, with only a 1.7% difference between the lateral and longitudinal creepage test results, which demonstrates the reliability and accuracy of V-Track for CoF

measurement. Further research may focus on reducing the uncertainty of longitudinal creepage measurement, especially at low creepage values, and investigating wheel-rail frictional rolling contact characterised by the measured creep curves.

References

[1] Fletcher, D. I., Lewis, S., "Creep Curve Measurement to Support Wear and Adhesion Modelling, Using a Continuously Variable Creep Twin Disc Machine," Wear, 298-299, 2013.

[2] Tanimoto, H., Chen, H., "Influence of Surface Roughness and Temperature on Wheel / Rail Adhesion in Wet Conditions," Quarterly Report of RTRI, 56(3), 2015.

[3] Zhang, W., Chen, J., Wu, X., Jin, X., "Wheel/Rail Adhesion and Analysis by Using Full Scale Roller Rig," Wear, 253(1-2), 2002.

[4] Li, Z., Arias-Cuevas, O., Lewis, R., Gallardo-Hernández, E. A., "Rolling–Sliding Laboratory Tests of Friction Modifiers in Leaf Contaminated Wheel–Rail Contacts," Tribology Letters, 33(2), 2009.

[5] Alonso, A., Guiral, A., Baeza, L., Iwnicki, S., "Wheel–Rail Contact: Experimental Study of the Creep Forces–Creepage Relationships," Vehicle System Dynamics, 52(sup1), 2014.

[6] Gutsulyak, D. V., Stanlake, L. J. E., Qi, H., "Twin Disc Evaluation of Third Body Materials in the Wheel/Rail Interface," Tribology - Materials, Surfaces & Interfaces, 15(2), 2021.

[7] Chang, C., Chen, B., Cai, Y., Wang, J.,"An Experimental Study of High – Speed Wheel-Rail Adhesion Characteristics in Wet Condition on Full Scale Roller Rig," Wear, 440-441, 2019.

[8] Boyacioglu, P., Bevan, A., Allen, P., Bryce, B., Foulkes, S., "Wheel Wear Performance Assessment and Model Validation Using Harold Full Scale Test Rig," Proceedings of the Institution of Mechanical Engineers, Part F: Journal of Rail and Rapid Transit, 236(4), 2022.

[9] Yang, Z., Zhang, P., Moraal, J., Li, Z., "An Experimental Study on the Effects of Friction Modifiers on Wheel–Rail Dynamic Interactions with Various Angles of Attack," Railway Engineering Science, 30(3), 2022.

[10] Liu, X., Xiao, C., Meehan, P. A., "The Effect of Rolling Speed on Lateral Adhesion at Wheel/Rail Inter-face Under Dry and Wet Condition," Wear, 438-439, 2019.

[11] Ren F., Yang Z., Hajizad O., Moraal J., Li Z., "Experimental investigation into the initiation of head check damage using v-track," in 12th International Conference on Contact Mechanics and Wear of Rail/Wheel Systems, 4-7 September 2022, Melbourne, Victoria, Australia, 2022.

[12] Naeimi, M., Li, Z., Petrov, R. H., Sietsma, J., Dollevoet, R., "Development of a New Downscale Setup for Wheel-Rail Contact Experiments Under Impact Loading Conditions," Experimental Techniques, 42(1), 2018.

[13] Zhang, P., Moraal, J., Li, Z., "Design, Calibration and Validation of a Wheel-Rail Contact Force Measurement System in V-Track," Measurement, 175, 2021.